RSC Advances

ROYAL SOCIETY OF CHEMISTRY

www.rsc.org/advances

The pseudo-graft copolymer micelle was constructed from the self-assembly of (6-(2-aminoethyl)-amino-6-deoxy)-cyclodextrin (β-CDen) modified poly(aspartic acid) (PASP-CD) with cholesterol-modified poly(D,L-lactide) (PLA-Chol) by host-guest inclusion complexation in water.

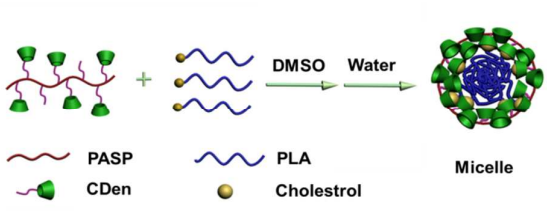

RSC Advances

RSCPublishing

ARTICLE

Construction of micelles based on biocompatible pseudo-graft polymers *via* β-cyclodextrin/cholesterol interaction for protein delivery

Cite this: DOI: 10.1039/x0xx00000x

Received ooth January 2012,
Accepted ooth January 2012

DOI: 10.1039/x0xx00000x

www.rsc.org/

Hui Han,[a] De-E Liu,[a] Hongguang Lu,[a] Wen-Xing Gu,[a] Hui Gao*[a]

A novel pseudo-graft copolymer was developed for protein delivery, based on the self-assembly of (6-(2-aminoethyl)-amino-6-deoxy)-cyclodextrin (β-CDen) modified poly(aspartic acid) (PASP-CD) with cholesterol-modified poly(D,L-lactide) (PLA-Chol) by host-guest inclusion complexation. The chemical structures of polymers were confirmed by Fourier transform infrared (FT-IR) spectroscopy and proton nuclear magnetic resonance (^{1}H NMR) spectroscopy. These components were then investigated for their ability to form nanoparticles and encapsulate protein. The diameter of micelles in water ranged from 70-200 nm as determined by dynamic light scattering, and the micelles were spherical in shape as observed by transmission electron microscopy. A model protein, bovine serum albumin (BSA), was encapsulated into the pseudo-graft copolymer micelles. The encapsulation efficiency (EE) and loading capacity (LC) of BSA in the micelles could be well tuned by the component of pseudo-graft copolymers. The micelles with a lower molar ratio of CD and cholesterol (hydrophilic/hydrophobic) exhibited a higher EE and LC. While *in vitro* release studies showed that a shorter chain of hydrophobic segment and higher hydrophilic/hydrophobic molar ratio could enhance release rate. Cell viability studies exhibited that these materials possessed good cell viability (> 95%). These results suggest that the degradable copolymers with proper hydrophilic and hydrophobic composition are able to self-assemble into micelles that are an effective and biocompatible vehicle for delivering protein, paving a new way for the application of pseudo-graft copolymer in protein or peptide delivery.

Introduction

Noncovalently connected micelles (NCCMs) are arousing interest of many researchers, probably due to the complicated polymerizing processes of conventional amphiphilic copolymers.[1,2] Only physical interactions rather than chemical bonds exist between shell and core in NCCMs, which are different from conventional polymeric micelles. Various types of non-covalent interactions, such as hydrogen bonding interactions,[3-5] metal-ligand interactions[6-8] and host-guest recognition[9-11] have been employed to construct supramolecular block or graft copolymers.[12] Compared to conventional polymers, the non-covalent nature of supramolecular copolymers endows them with enhanced structural versatility, flexibility, tunability,[13] robust combination of different building blocks and adaptability to external stimulus.[14]

Cyclodextrins (CDs), as a good candidate to build NCCMs, are a series of natural cyclic oligosaccharides composed of 6, 7, or 8 D-(+)-glucose units linked by α-1,4-linkages, and named α-, β-, or γ-CD, respectively.[15] The geometry of CDs gives a hydrophobic inner cavity having a depth of ca. 7.0 Å, and an internal diameter of ca. 4.5, 7.0, and 8.5 Å for α-, β-, or γ-CD, respectively. The hydrophobic interior cavity of β-CD can accommodate a variety of guest molecules, such as adamantane (AD),[16-18] adamantinecarboxylic acid (ACA)[19] and cholesterol,[20,21] AZO,[22] ferrocene,[23] and so on, to form supramolecular inclusion complexes.[24-26] In addition, CDs have been chosen as drug carriers since 1950s, because of their bioavailability and low toxicity.[27] A lot of developments of drug delivery systems based on CDs have been investigated by us and others in recent years, which were for biomedical and pharmaceutical applications,[28-30] especially for peptide and protein delivery.[32-34] However, the study of pseudo-graft copolymer based on β-CD/cholesterol inclusion complexes to form nanoparticles as a protein delivery system has not been given.

The supramolecular guest used in this work was poly(D,L-lactide) (PLA) bearing a cholesterol end (PLA-Chol). The cholesterol moiety was chosen because cholesterol is important in the stability of lipid rafts, bearing interaction sites for membrane receptors.[35] PLA was selected as the hydrophobic core-forming moiety due to its excellent biocompatibility, which has been widely used in the fields of protein delivery and tissue engineering.[32,36-37] (6-(2-aminoethyl)-amino-6-deoxy)-cyclodextrin (β-CDen) grafted poly(aspartic acid) (PASP-CD) was prepared as the supramolecular host. Recently, PASP as a polyamion acid polymer has attracted a great deal of attention as a biocompatible and water-soluble materials to being a

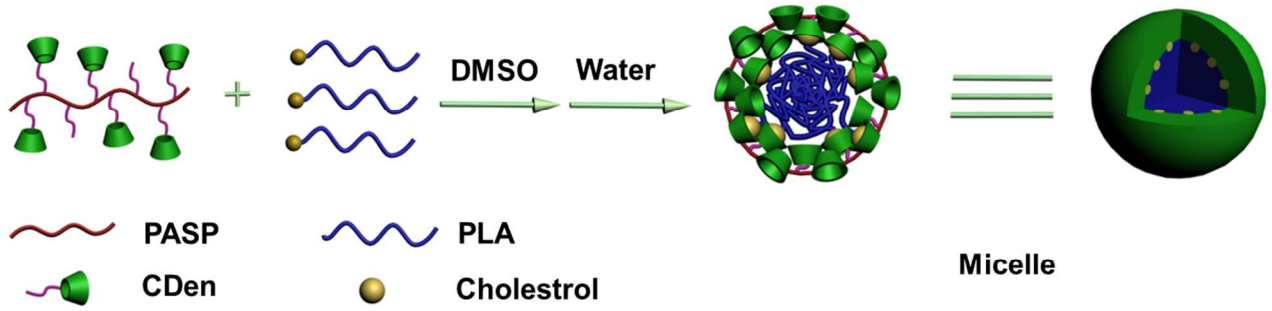

Scheme 1 Schematic representation of the formation of pseudo-graft copolymer from PASP-CD and PLA-Chol in water, driven by host-guest interaction complextion.

candidate of drug carrier in biomedical applications.[38] In particular, PASP-based nanoparticles,[39,40] micelles,[41,42] nanocapsules[43] and membranes[44] were fabricated for the delivery of drug, DNA, RNA and proteins.

Herein, we present a novel protein delivery system comprising a PASP-CD polymer which forms supramolecular self-assembly micelles with different molecular weights of PLA-Chol through host-guest inclusion complexation in water (Scheme 1). Micelles composed of pseudo-graft copolymers were fabricated using the dialysis method and were used for encapsulate a model protein, *i.e.*, bovine serum albumin (BSA). The size, morphology, colloidal stability, cell viability of the micelles were studied, and the encapsulation efficiency, release profiles of BSA-loaded micelles with different PASP-CD and PLA-Chol molar ratio and different molecular weight of PLA-Chol were also investigated.

Experimental sections

Material and techniques

Stannous octoate ($Sn(Oct)_2$) was purchased from Sigma-Aldrich Co., Ltd. (Shanghai,China). D,L-lactide and 8-anilino-1-naphthalene sulfonate (ANS) were purchased from Heowns biochem technologies Co., Ltd. (Tianjin, China). Cholesterol was purchased from Best Reagent Co., Ltd. (Chengdu, China). Bovine serum albumin (BSA) was purchased from Aladdin reagent Co., Ltd. (Shanghai, China). L-aspartic acid (L-Asp, 99%) was purchased from Alfa Aesar Co., Ltd. (Beijing, China). Tetramethylene sulfone was purchased from J&K Scientific Co., Ltd. (Beijing, China). Mesitylene, ethanediamine (EDA), dimethylfomamide (DMF), *β*-cyclodextrin (*β*-CD, 98%), *p*-toluenesulfonyl chloride and other reagents were purchased from Tianjin Chemical Reagent Co., Ltd. (Tianjin, China). Cholesterol was purified by recrystallization from acetone. *p*-toluenesulfonyl chloride was purified by recrystallization from a mixture of n-hexane and benzene. *β*-CD was used after recrystallization from water and drying under vacuum. DMF and EDA were distilled before use. All other reagents were used as received.

The FT-IR spectra of CDen, poly(succinimide) (PSI) and PASP-CD were recorded using KBr discs on a spectrometer (Bio-Rod 6000, Thermo Electron, USA) at room temperature. All ^{1}H NMR spectra were recorded on a NMR spectrometer (AV-400, Bruker, Freemont, CA) at room temperature with $CDCl_3$, D_2O and DMSO-d_6 as the solvents, respectively. The number average molecular weight (Mn) and molecular weight distribution (Mw/Mn) of PSI and PLA-Chol were determined with gel permeation chromatography (GPC) (R1-201H, Shoko Scientific Co., Ltd., Japan), equipped with DMF and tetrahydrofuran (THF) as the mobile phase and polystyrene was used as calibration standard.

Synthesis of polymers

Synthesis of mono-6-deoxy-6-(p-tolylsulfonyl)-cyclodextrin (Mono-6-OTs-*β*-CD) Mono-6-OTs-*β*-CD was synthesized according to the previous report.[45] Briefly, NaOH solution was added dropwise to a suspension of the *β*-CD in water. The mixture was stirred in ice-water bath, while *p*-toluenesulfonyl chloride in acetonitrile was added dropwise. After 5 h of stirring in ice bath, the unreacted *p*-toluenesulfonyl chloride was removed by suction filtration, and the filtrate was adjusted with HCl solution to be approximately pH = 6 and refrigerated overnight. The white crystal product was recovered by suction filtration and the purified product was dried in a vacuum oven at 50 °C for 3 days (Yield: 20%).

Synthesis of *β*-CDen *β*-CDen was synthesized according to the previously reported method.[46] 6.0 g of mono-6-OTs-*β*-CD was reacted with excess amount of EDA (36 mL) at 75 °C for 4.5 h, and then cooled to room temperature. Subsequently, 30 mL of cold acetone was added into the mixture, and white precipitate formed immediately. After the precipitate was collected by suction filtration, the precipitate was repeatedly dissolved in 30 mL of water-methanol mixture and poured into a large amount of cold acetone several times to remove unreacted EDA. The product was dried at 50 °C for 3 days in a vacuum oven (Yield: 75%).

Synthesis of PSI PSI was synthesized according to a previous report.[47] L-Aspartic acid (25 g, 188 mmol), 85% phosphoric acid (2 g, 17.34 mmol) and the mixture solution (mesitylene/sulfolane = 56 g/24 g) were mixed in a three-neck round-bottom flask. The mixture solution was refluxed under nitrogen atmosphere at 180 °C, and the water formed in the reaction process was removed using the Dean-Stark trap with a reflux condenser. The reaction was processed for 4.5 h. After the reaction mixture was cooled down, the solvent was removed. Then DMF was added to dissolve the polymer, and precipitated into excess methanol twice. After filtration, the precipitate was washed several times with distilled water to remove the phosphoric acid. The product was finally dried at 80 °C in a vacuum for three days to obtain PSI in white powder (Yield: 85%).

Synthesis of PASP-CD PASP-CD was synthesized by the ring-opening reaction of PSI with *β*-CDen.[48] PSI (1 mmol) was dissolved in DMF (10 mL), and the solution was stirred in an

ice-water bath under nitrogen, followed by addition of the β-CDen (3 g, 2.5 mmol) in 30 mL of DMF. The reaction mixture was heated to 60 °C and stirred for 3 days. The product was precipitated in ether. After filtration, the precipitate was dissolved in DMF, then dialyzed (Mw cut-off = 10-12 kDa) against deionized water at 0-5 °C for 3 days, and then freeze-dried (Yield: 80%).

Synthesis of PLA-Chol

13.96 g (96.94 mmol) of D,L-lactide was polymerized under vacuum using 0.04 g (0.1 mmol) of $Sn(Oct)_2$ as a catalyst and 1.18 g (3.05 mmol) of cholesterol as an initiator. The reaction was maintained at 150 °C for 5 h in bulk. The solid product was dissolved in acetone, and precipitated in deionized water. The product was filtered and dried in a vacuum oven at 50 °C (Yield: 55%).

Preparation of micellar solutions and BSA-loaded micellar solutions

Micellar solutions were prepared using dialysis method from PLA-Chol of different molecular weights (The Mn of PLA-Chol was 5 kDa, 10 kDa, 15 kDa, respectively, and named as PLA-Chol1, PLA-Chol2, PLA-Chol3) and PASP-CD with molar ratio (cholesterol/CD) of 1:1, 1:2, 1:3, 1:4. In a typical example, to prepare $M_{15K}1$ ("M" represents "micelles", "15K" represents the molecular weight of PLA-Chol and "1" represents the molar ratio of CD and cholesterol), 4 mg of PASP-CD with an equivalent molar (1:1 cholesterol/CD molar ratio) of PLA-Chol3 (10 mg) were dissolved in DMSO (10.0 mL). After vigorous stirring for 5 h, the mixture was added to 5 mL of deionized water or aqueous solution of BSA (for preparing BSA-loaded micellar solutions) *via* a syringe pump at a flow rate of 0.5 mL/min, and the dispersion was left stirring for another 5 h at room temperature. DMSO was then removed by dialysis (Mw cut-off = 12 kDa) against deionized water for 3 days. Stock solutions with a characteristic bluish tinge were obtained.

Particle size analysis and morphology examination

Micellar particle size was determined in water at 25 °C by DLS on a Zetasizer Nano (ZS90, Malvern Instruments, Southborough, MA). Then the variation of particle size at different pH was also measured using DLS. The pH values of the stock solutions were adjusted with 0.1 M NaOH or HCl.

Transmission electron microscopy (TEM) was conducted on an instrument (Jeol-1400, Jeol, Japan) with an accelerating voltage of 100 kV. Samples were prepared by dropping two drops of the micellar solutions (0.1 mg mL^{-1}) onto a carbon coated copper grid and dried.

ANS fluorescence measurements of PSAP-CD and micellar solutions

ANS stock solution was added into 3 mL of the micellar solution, stirred for 2 h, and sonicated for 20 min before measurements. The final ANS concentration was set as 0.05 mM. The fluorescence emissions of these solutions were recorded at an excitation wavelength of 370 nm using a spectrofluorophotometer (F-7000, Hitachi, Japan).

Determination of the encapsulation efficiency (EE) and the loading capacity (LC) of BSA

5 mL of BSA-loaded micelles were centrifuged at 22000 rpm (4 °C) for 40 min. The EE and LC were determined by measuring the BSA concentration in the supernatant, which was measured according to the blue coomassie G250 protein assay.[49] The UV-vis absorbance (Persee, TU-1900, Beijing) was recorded at the 595 nm. The LC and EE were calculated from the following equation:

$$\text{Initial loading (\%w/w)} = \frac{\text{Mass of initial BSA}}{\text{Mass of (initial BSA+polymers)}} \times 100\%$$

$$\text{LC (\%w/w)} = \frac{\text{Mass of loaded BSA}}{\text{Mass of nanoparticles}} \times 100\%$$

$$\text{EE (\%)} = \frac{\text{LC}}{\text{Initial loading}} \times 100\%$$

Release of BSA from micelle

9 mL of BSA-loaded micelles were incubated in a capped centrifuge tube containing 1 mL of phosphate buffered saline (PBS; pH = 7.4). The centrifuge tube was kept in a thermostatic water bath oscillators (Xinhang Instrument, SHZ-82, Jintan) at 37 °C and shaken at 120 rpm. At appropriate intervals, 1 mL of the supernatant was sampled and an equal amount of fresh PBS was added to the tube. The samples were centrifuged at 22000 rpm for 40 min. The BSA concentration in the supernatant was determined as described above. Each experiment was repeated three times and the result was the mean value of the three measurements.

Circular dichroism spectra of BSA samples

The circular dichroism measurements of free BSA in the release medium and control BSA solutions in water were performed on a Jasco-715 spectropolarimeter at 20 °C using the matched 10 mm path length quartz cells. Each sample solution was scanned in the range of 190–250 nm. A circular dichroism spectrum was recorded as the average value of three scans.

Cell viability assays

Cell viability was detected using Cell Counting Kit-8 (CCK8) assay. Mouse fibroblast cells (L929) were cultivated in a humidified 5% carbon dioxide atmosphere at 37 °C on a 96-well microplate, with 5,000 cells immersed in complete growth medium per well. The cells with 100 μL of RPMI-1640 per well were allowed to attach for 24 h. Subsequently, the copolymer suspensions at the PASP-CD concentrations of 0.1, 0.3, 0.5, 0.7, and 0.9 mg mL^{-1} were added to 96-well plates at 10 μL per well and incubated for 24 h, respectively. The solution was then removed and replaced with 100 μL of RPMI-1640. Then, CCK-8 solution was added to 96-well plates at 10 μL per well and incubated for 24 h, and the resulting solution

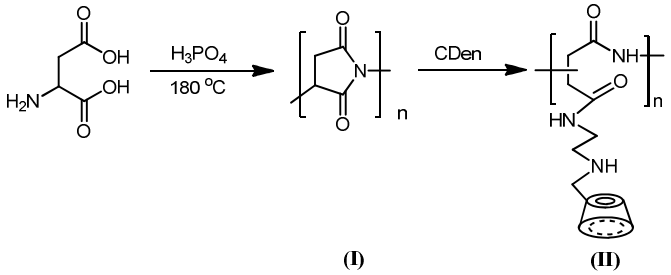

(I) (II)

Scheme 2 Synthesis of PSI (I) and PASP-CD (II).

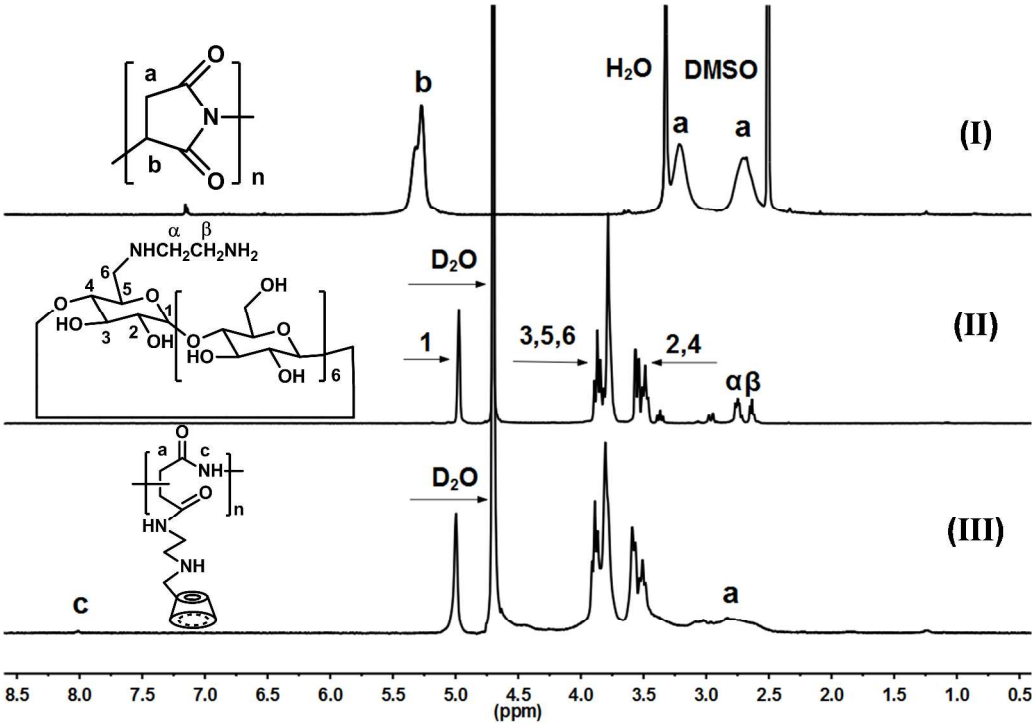

Fig. 1 ^{1}H NMR spectra of PSI (I) in DMSO-d_6, β-CDen (II) and PASP-CD (III) in D_2O.

was analyzed at 450 nm by means of a plate reader with a background correction using a Bio-Tek FLx800 Fluorescence Microplate Reader. This process was repeated for eight times in parallel. The results are expressed as the relative cell viability (%) with respect to control wells.

Results and discussion

Synthesis and characterization of PASP-CD

Scheme 2 exhibits the synthetic procedure of PSI and PASP-CD. PASP-CD was synthesized by the ring-opening reaction of PSI with β-CDen. The molecular weight of PSI measured by GPC was 2.2 × 104 with polydispersity index (PDI) of 1.47.

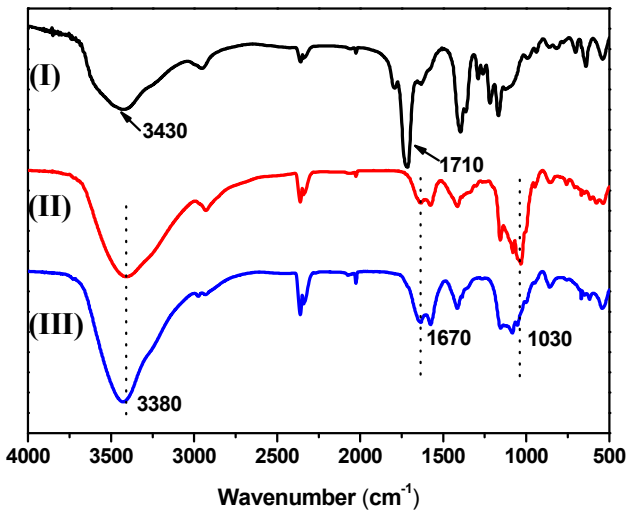

Fig. 2 FT-IR spectra of PSI (I), CDen (II) and PASP-CDen (III).

The ^{1}H NMR spectra of PSI, as well as β-CDen in Fig. 1 indicated the successful synthesis of PSI and β-CDen. While the ^{1}H NMR spectrum of PASP-CD in Fig. 1 (III) showed the disappearance of the peak located at 5.30 ppm, which was assigned to methine protons (peak "b") of succinimide units, indicated that the ring-opening of PSI completed. In addition, the peak "c" located at 8.0 ppm in Fig. 1 (III) assigned to amide groups was observed.[47] Fig. 2 shows the FT-IR spectra of PSI, β-CDen and PASP-CD. In the FT-IR spectrum of PSI (Fig. 2 (I)), the peak at 1710 cm^{-1} is attributed to the carbonyl from cyclic imides stretching. The peaks located at 3380 cm^{-1} and 1030 cm^{-1} arised from multihydroxyl groups of the β-CDen (Fig. 2 (II) & (III)). Especially, the characteristic carbonyl groups from cyclic imides stretching located at 1710 cm^{-1} (Fig. 2 (I)) was absence in Fig. 2 (III), and a new peak located at 1670 cm^{-1} appeared, assigned to the stretching vibration of carbonyl in the amide groups on the PASP-CD, indicating that the aminolysis of PSI completed.

Synthesis of PLA-Chol

End-functionalized polymers can be synthesized *via* direct

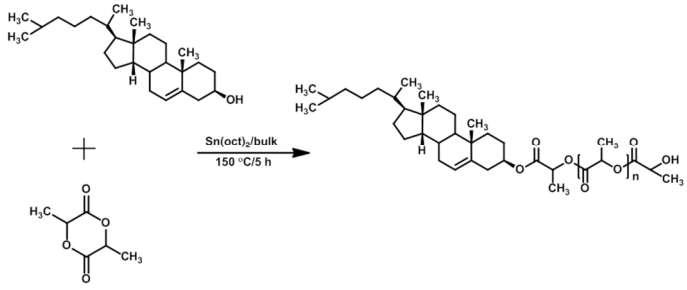

Scheme 3 Synthesis route of PLA-Chol.

Table 1 Molecular weight of PLA-Chol

	Mn (Theory)	Mn (^{1}H NMR)[a]	Mn (GPC)[b]	Mw/Mn[b]	Yield %
PLA-Chol1	5000	4800	5300	1.21	46.3
PLA-Chol2	10000	9900	9300	1.32	50.5
PLA-Chol3	15000	14400	17500	1.35	55.6

[a]Determined by ^{1}H NMR.
[b]Determined by GPC using polystyrene as standards.

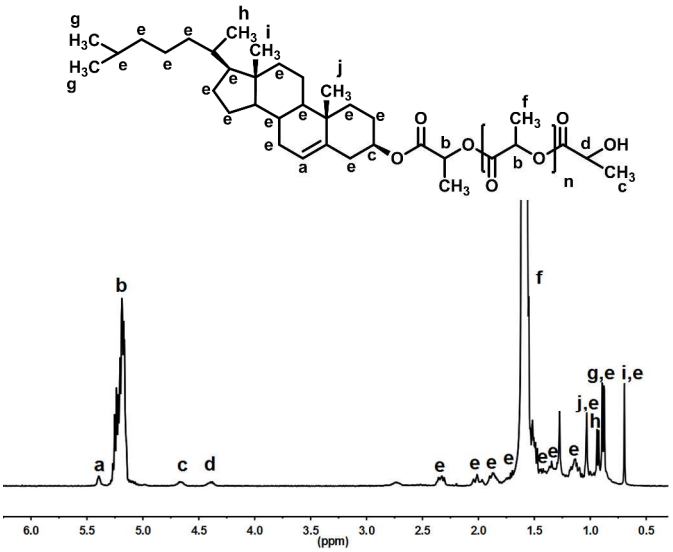

Fig. 3 ^{1}H NMR spectrum of PLA-Chol in $CDCl_3$.

polymerization using a functional initiator[50,51] or through the post-modification of polymers with reactive terminal moieties.[51,52] The polymerization of lactide in the presence of hydroxy functionality-containing compound with $Sn(Oct)_2$ as the catalyst has been reported by several investigators.[53] The preparation route of PLA-Chol is illustrated in Scheme 3. The molecular weight of PLA-Chol was adjusted by varying the D,L-lactide/cholesterol ratio. The polymer composition and molecular weight were characterized by ^{1}H NMR and GPC (Table 1). Fig. 3 shows the ^{1}H NMR spectrum of PLA-Chol. The multi peaks appeared between 0.67-2.33 ppm were assigned to the -CH_2, -CH_3 in cholesterol and -CH_3 in D,L-lactic acid units (e, f, g, h, i). The peak "b" at 5.21 ppm assigned to the O=C-CH-O in D,L-lactic acid units. The peak "a" at 5.37 ppm was assigned to the -CH=C in cholesterol, suggesting that the double C=C was not destroyed during the polymerization. The number-average molecular weight of PLA-Chol was determined from the integrals ratio of the peak "b" at 5.21 ppm and the peak "c" at 4.64 ppm (-CH groups in the cholesterol moiety which neighbors the PLA block) (Table 1). The molecular weights obtained from ^{1}H NMR and GPC were in good agreement with the theoretical molecular weights.

Table 2 Characteristics of micelles composed of PASP-CD and PLA-Chol.

Micelles	Host/Guest[a]	Diameter[b] (nm)	PDI[b]	Diameter[c] (nm)	PDI[b]
$M_{15K}1$	1:1	70.5	0.143	64.7	0.279
$M_{15K}2$	2:1	85.0	0.107	65.3	0.197
$M_{15K}3$	3:1	102.2	0.118	70.4	0.191
$M_{15K}4$	4:1	211.3	0.228	92.5	0.283
$M_{10K}1$	1:1	66.1	0.379	-	-
$M_{10K}2$	2:1	72.0	0.260	84.0	0.235
$M_{10K}3$	3:1	98.0	0.203	-	-
$M_{10K}4$	4:1	124.9	0.193	-	-
$M_{5K}1$	1:1	119.2	0.269	-	-
$M_{5K}2$	2:1	172.4	0.255	154.0	0.219
$M_{5K}3$	3:1	197.4	0.205	-	-
$M_{5K}4$	4:1	219.5	0.206	-	-

[a] The molar ratio of CD in PASP-CD and cholestol in PLA-Chol.
[b] The diameter and PDI of micelles in water.
[c] The diameter and PDI of BSA-loaded micelles in water.

Micellar behavior of pseudo-graft copolymer

Inspired by the work of Jiang *et al*,[54] we prepared the pseudo-graft copolymer in DMSO first, followed by the addition of water to induce self-assembly, and the subsequent dialysis to remove DMSO. After dialysis, a stable dispersion with a bluish tinge formed. The micellar solutions exhibited no macroscopic phase separation upon standing at room temperature for more than three weeks, suggesting the formation of stable aggregates. The diameters of the complexes were in the range of 70-200 nm as determined using DLS (Table 2). The particle size decreased with increased ratio of hydrophobic moiety, or higher molar ratio of hydrophobic PLA-Chol. It has been reported that, the hydrophobic segment could promote the core compactness of micelles, and enlarged amount of hydrophobic portion could result in the formation of smaller particles in aqueous solutions.[55] DLS measurements were then performed at different pH (Fig. 4). The particles were stable at neutral or alkaline environment (pH $>$ 5) while the size became larger rapidly (about 400 nm) at acid environment (pH $<$ 5), even precipitated at pH lower than 3. The solvation effects, as attracting forces between polymer and solvent molecules could promote the dissolution of polymer. The solvation effects of

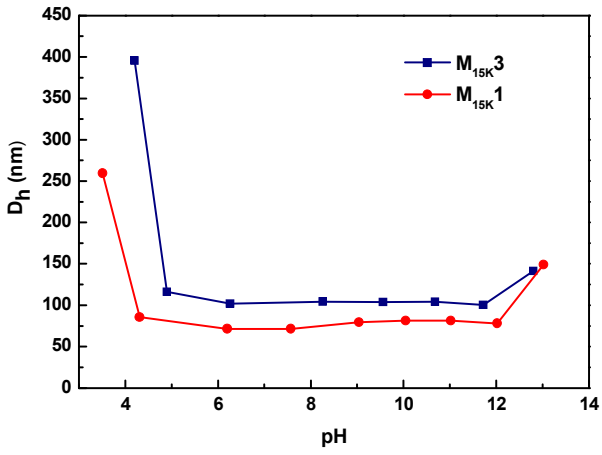

Fig. 4 The diameter of $M_{15K}1$ and $M_{15K}3$ at different pH.

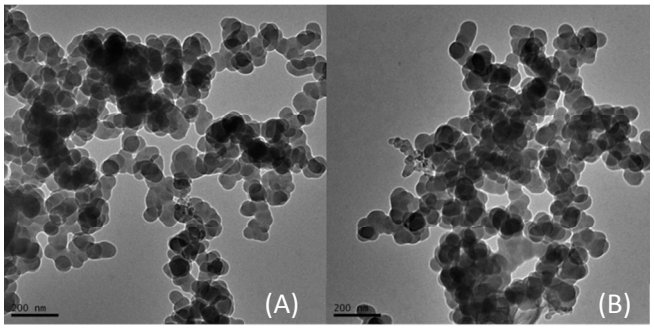

Fig. 5 TEM image of $M_{15K}1$ (A) and $M_{10K}2$ (B).

PASP-CD at different pH influenced the particle size of the micelles. Lowering the pH led to the protonation of amino group in PASP-CD, and resulted in the solvation effects. With the augmentation of the solvation, the micelles swelled, causing an enlarged particle size. Finally, the hydrophilic PASP-CD was unable to stabilize the hydrophobic core. As a result, hydrophobic PLA-Chol was separated from water and precipitated. $M_{15K}3$ and $M_{15K}1$ exhibited a similar trend curve. The morphology of these micelles in water was observed using TEM (Fig. 5). The micelles were spherical in shape with a diameter of approximately 50 nm. The size observed from TEM was smaller than that measured by DLS (70 nm) due to the dry nature of the TEM samples (*i.e.*, polymer solvent swelling is absent).

^{1}H NMR analysis of the complex

In order to explore the possible interaction of the PASP-CD/PLA-Chol complex, we compared the ^{1}H NMR spectra of PASP-CD and the inclusion complex in D2O (Fig. 6). Owing to its poor water solubility, the proton signal of cholesterol is invisible in 1H NMR under most conditions when D2O is used as a solvent. However, in the present of PASP-CD, assessment of the complex by 1H NMR clearly demonstrated the presence of the framework protons of the cholesterol molecule. As illustrated in Fig. 6, the cholesterol protons displayed chemical shifts at 1.2-1.7 ppm (peak "a"). In addition, after complexation with PLA-Chol, the chemical shifts of β-CD (H-1, H-2 protons)

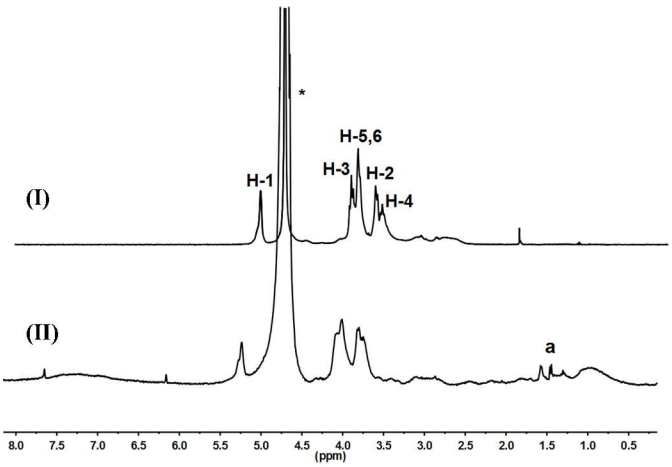

Fig. 6 ^{1}H NMR spectra of PASP-CD (I) and PASP-CD/PLA-Chol complex (II) in D2O (asterisk highlights the water peak).

Table 3 The chemical shifts (δ) of PASP-CD and PASP-CD/ PLA-Chol complex.

CD		δ (ppm)	
		PASP-CD	PASP-CD/PLA-Chol Complex
H1	d	4.990	5.230
H2	dd	3.561	3.793
H3	dd	3.880	4.073
H4	dd	3.502	3.739
H5, H6	m, dd	3.798	4.002

in PASP-CD exhibited the significant changes (0.19-0.24 ppm) (Fig. 6, Table 3). It is noteworthy that H-5 protons shifted ca. 0.204 ppm, but H-3 protons showed relatively weak shifts (0.193 ppm) in the complex. Both H-3 and H-5 protons are located in the interior of β-CD cavity. H-3 protons are near the wide side of cavity, while H-5 protons near the narrow side, indicating that cholesterol probably penetrated into the β-CD cavity from the narrow side.

ANS fluorescence

The loading behavior of the micelles was studied using fluorescent chromophore 8-anilino-1-naphthalene sulfonate (ANS) as a model guest. The fluorescent characters of ANS largely depend on its microenvironment, and an apparent intensity increase and peak blue shift can be observed when ANS molecules move from water to the *β*-CD cavities.[56] We first measured the fluorescence emission of ANS in water containing PASP-CD with different concentrations (Fig. 7 (I)). The intensity and the blue shift of the ANS emission increased with the concentration of the PASP-CD. When the *β*-CD molar content in the solutions was equal to that of ANS (5×10^{-5} M), the emission intensity increased 4 times and the peak shifts from 522 to 492 nm. Similar fluorescence experiments were performed for the solutions of ANS with the PASP-CD/PLA-Chol micelles. As shown in Fig. 7 (II), compared to the blank solution of ANS in water, all the micellar solutions of $M_{15K}1$, $M_{15K}2$, $M_{15K}3$ and $M_{15K}4$ caused an apparent increase in the emission intensity and a small blue shift of the emission peak of ANS, which indicated that the residue CD cavities in the micelles have the ability to accommodate the ANS molecules. Furthermore, the effects of the micelles on the emission behavior of ANS were clearly intensified when the molar ratio of *β*-CD to cholesterol increased from 1 to 4 for M_{15K}. More residue *β*-CD cavities are available as the increase in the molar ratio of *β*-CD to cholesterol in the micelles from $M_{15K}1$ to $M_{15K}4$. However, no obviously blue shift could be observed between the micelles. ANS, as a hydrophobic probe, probably got into the inner hydrophobic core of the micelles. Consequently, the fluorescence intensity of ANS enhanced due to the microenvironment change.

EE and LC of BSA in the micelles

The EE and LC of BSA in the micelles were calculated from UV detection, and the data were listed in Table 4. The LC (17%-32%) and EE (34%-62%) of pseudo-graft copolymer micelles were close to the conventional nano-carrier. It appeared that the orders in the EE and LC were as following: M15K2 > M10K2 > M5K2; M15K1 > M15K2 > M15K3 > M15K4. The BSA loading was enhanced as a result of a relatively strong hydrophobic interaction between polymer and BSA. BSA contain hydrophobic groups, such as aromatic groups and some large alkyl groups, which could interact with

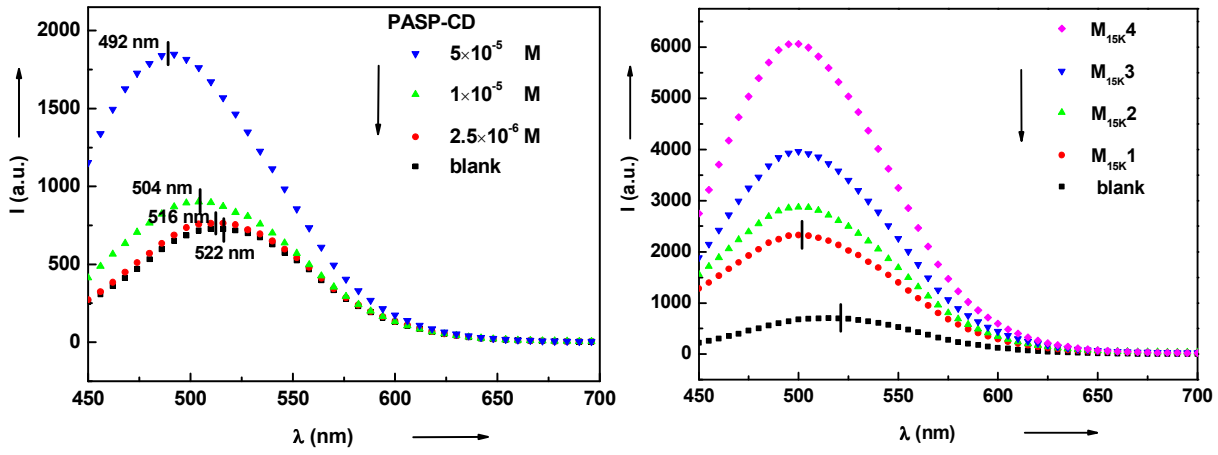

(I) (II)

Fig. 7 Fluorescence spectra of ANS in water (black) and in PASP-CD solutions with different concentrations as indicated in (I) and ANS in $M_{15K}1$ (red), $M_{15K}2$ (green), $M_{15K}3$ (blue), and $M_{15K}4$ (pink) solutions (II). The β-CD molar concentrations (in 1×10^{-5} M) are 1.5 ($M_{15K}1$), 3.6 ($M_{15K}2$), 7.0 ($M_{15K}3$), and 12.6 ($M_{15}4$). The bottom curve is for ANS in water; ANS concentration is 5×10^{-5} M. The excitation wavelength is 370 nm, and the emission was recorded from 450 to 700 nm.

Table 4 Encapsulation efficiency (EE) and loading capacity (LC) of micelles.

Micelles	LC (%)	EE (%)
$M_{15K}1$	31.2	62.4
$M_{15K}2$	30.2	60.4
$M_{15K}3$	26.9	53.8
$M_{15K}4$	23.8	47.6
$M_{10K}2$	24.2	48.5
$M_{5K}2$	17.1	34.2

the hydrophobic moiety of the polymer, and can enhance the EE and LC of BSA.[57] Therefore, the hydrophilic/hydrophobic balance of the pseudo-graft copolymer influenced the EE and LC. At the same molar ratio of β-CD/cholesterol of 1:2, a longer chain of hydrophobic segment (M15K2 > M10K2 > M5K2) of the pseudo-graft copolymer facilitates the chain coiling, resulting in the enhanced BSA loading. In addition, as the molar ratio of cholesterol/β-CD varied from 1 to 4 for M15K, the micelle composed of more PASP-CD hydrophilic segment exhibited decreased EE and LC.

In vitro BSA release from the micelles

Fig. 8 shows the release curves of BSA from the micelles in PBS (pH = 7.4). All micelles formulations can release 45-85% of BSA within 10 h, and then reach a plateau. The release rate could be well tuned by the composition of the pseudo-graft copolymers. The release rates of the BSA accumulative release were almost contrary to the LC and EE of BSA. The release of protein occurs predominantly by diffusion of the drug through aqueous pores generated in the dosage form, which is associated with generation of micropores in the degradation and enhanced water uptake.[58] β-CDs could probably offer channels for the BSA diffusion. Therefore, the micelles with more residue β-CD (at lower cholesterol/β-CD ratio) release its cargo faster. Additionally, the hydrophobicity of the micelles increased with the molecular weight of PLA-Chol, which contributed to induce a compact structure, and thus the

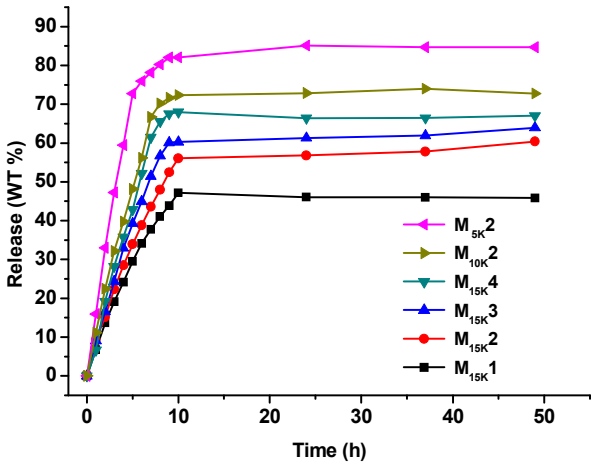

Fig. 8 *In vitro* release curves of BSA from micelles in PBS.

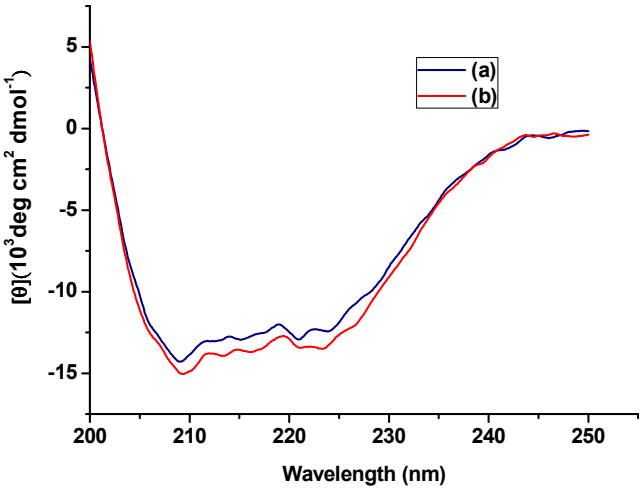

Fig. 9 Circular dichroism spectra of the BSA solutions. (a) Native BSA, (b) BSA released after 2 days from the $M_{15K}3$.

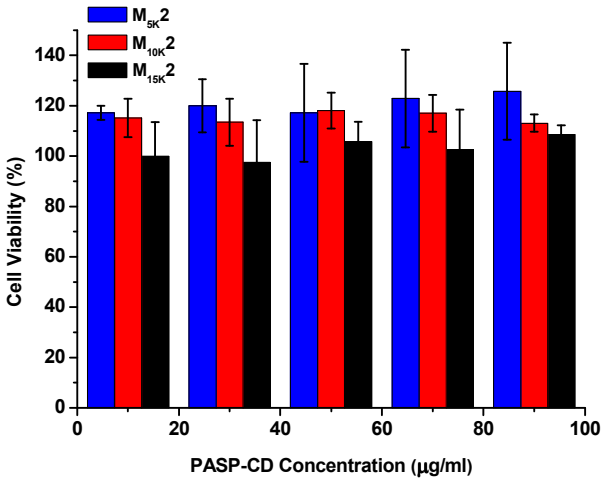

Fig. 10 Cell viabilities of polymer complexes against L929 cells. The cells were treated with increasing concentrations of PASP-CD in copolymers, incubated for 24 h before analysis by CCK8 assay.

cumulative release decreased with the increased PLA-Chol molecular weight. The release result exhibited that the protein can be released effectively and the copolymer micelles has the ability to be used as a potential protein carrier.

Circular dichroism (CD) spectroscopy is a common method to analyze the secondary structure of a protein with high reliability. The CD spectra of the free BSA in the supernatant from the release test after 2 days were measured and shown in Fig. 9. Obviously, two extreme valleys at 208 and 222 nm occurred without any significant difference from those of the native BSA. The result indicated that the released BSA remained its original structure due to the mild encapsulation condition.

Cell viability assays

The *in vitro* cytotoxicity of the host/guest complexes are an extremely important factor for their consideration as a safe protein vector. In this work, the *in vitro* cytotoxicity of the freeze-dried powder of $M_{15K}2$, $M_{10K}2$, $M_{5K}2$ were evaluated using CCK8 assays against L929 cells as a function of the concentrations (Fig. 10). All the samples retained high cell viability (> 95%) after 24 h of incubation at all tested concentrations up to 90 μg mL^{-1}. Some average cell viabilities were a little bit larger than 100% (about 120%) in Fig. 10, probably due to the experimental error of the data. Their low cytotoxicity further highlighted the advantage of the copolymers as the desirable drug carrier.

Conclusions

In summary, well-defined PASP-CD and PLA-Chol of different molecular weights were synthesized and characterized. A novel and efficient protein cargo based on the supramolecular pseudo-graft copolymer has been developed *via* the self-assembly of PASP-CD with different molecular weight of PLA-Chol by host-guest inclusion complexation. The ANS fluorescence measurement revealed the possible mechanism of micelles formation. The particle size, EE, LC and release process can be well tuned by adjusting the pseudo-graft copolymer composition. A shorter chain of hydrophobic segment and higher hydrophilic/hydrophobic led to an enlarged partical size and a less EE and LC, as well as an enhanced release rate. Additionally, the released BSA could maintain its native secondly structure. These complexes, with flexible composition and good biocompatibility, are capable of being efficient protein delivery vehicles.

Acknowledgements

Financial support from National Natural Science Foundation of China (21374079), Program for New Century Excellent Talents in University (NCET-11-1063), Program for Prominent Young College Teachers of Tianjin Educational Committee is highly acknowledged.

Notes and references

[a] *School of Chemistry and Chemical Engineering, Tianjin Key Laboratory of Organic Solar Cells and Photochemical Conversion, Tianjin University of Technology, Tianjin 300384, China.*
Fax: (+ 86) 2260214251; Tel: (+ 86) 2260214259; H. Gao, E-mail: ghhigher@hotmail.com, hgao@tjut.edu.cn.

1 M. Y. Guo and M. Jiang, *Soft Matter*, 2009, **5**, 495-500.
2 D. Y. Chen and M. Jiang, *Acc. Chem. Res.*, 2005, **38**, 494-502.
3 X. W. Yang, F. J. Hua, K. Yamato, E. Ruckenstein, B. Gong, W. Kim and C. Y. Ryu, *Angew. Chem. Int. Ed.*, 2004, **43**, 6471-6474.
4 W. H. Binder, S. Bernstorff, C. Kluger, L. Petraru and M. J. Kunz, *Adv. Mater.*, 2005, **17**, 2824-2828.
5 T. Park and S. C. Zimmerman, *J. Am. Chem. Soc.*, 2006, **128**, 11582-11590.
6 M. Chiper, M. A. R. Meier, D. Wouters, S. Hoeppener, C. A. Fustin, J. F. Gohy and U. S. Schubert, *Macromolecules*, 2008, **41**, 2771-2777.
7 B. G. G. Lohmeijer, D. Wouters, Z. H. Yin and U. S. Schubert, *Chem. Commun.*, 2004, **24**, 2886-2887.
8 J. M. Pollino, L. P. Stubbs and M. Weck, *J. Am. Chem. Soc.*, 2004, **126**, 563-567.
9 J. Wang and M. Jiang, *J. Am. Chem. Soc.*, 2006, **128**, 3703-3078.
10 U. Rauwald and O. A. Scherman, *Angew. Chem. Int. Ed.*, 2008, **47**, 3950-3953.
11 F. Huang, D. S. Nagvekar, C. Slebodnick and H. W. Gibson, *J. Am. Chem. Soc.*, 2005, **127**, 484-485.
12 R. Hoogenboom, D. Fournier and U. S. Schubert, *Chem. Commun.*, 2008, **2**, 155-162.
13 G. S. Chen and M. Jiang, *Chem. Soc. Rev.*, 2011, **40**, 2254-2266.
14 H. Liu, Y. F. Zhang, J. M. Hu, C. H. Li and S. Y. Liu, *Macromol. Chem. Phys.*, 2009, **210**, 2125-2137.
15 J. Szejtli, *Chem. Rev.*, 1998, **98**, 1743-1753.
16 M. V. Rekharsky and Y. Inoue, *Chem. Rev.*, 1998, **98**, 1875-1917.
17 M. Y. Guo, M. Jiang, and G. Z. Zhang, *Langmuir*, 2008, **24**, 10583-10586.
18 Mingming Zhang, Meijuan Jiang, Luyan Meng, Keyin Liu, Yueyuan Mao and Tao Yi, *Soft Matter*, 2013,**9**, 9449-9454.
19 D. Harries, D. C. Rau and V. A. Parsegian, *J. Am. Chem. Soc.*,

2005, **127**, 2184-2190.
20 R. Breslow and B. Zhang, *J. Am. Chem. Soc.*, 1996, **118**, 8495-8496.
21 K. Akiyoshi, A. Ueminami, S. Kurumada and Y. Nomura, *Macromolecules*, 2000, **33**, 6752-6756.
22 Y. Wang, M. Zhang, C. Moers, S. Chen, H. Xu, Z. Wang, X. Zhang and Z. Li, *Polymer*, 2009, **50**, 4821-4828.
23 Q. Yan, J. Y. Yuan, Z. N. Cai, Y. Xin, Y. Kang and Y. W. Yin, *J. Am. Chem. Soc.*, 2010, **132**, 9268-9270.
24 G. Wenz, B. H. Han and A. Muller, *Chem. Rev.*, 2006, **106**, 782-817.
25 A. Harada, *Acc. Chem. Res.*, 2001, **34**, 456-464.
26 Y. Liu, Y. W. Yang, Y. Chen and H. X. Zou, *Macromolecules*, 2005, **38**, 5838-5840.
27 K. Uekama, F. Hirayama and T. Irie, *Chem. Rev.*, 1998, **98**, 2045-2076.
28 N. Yui and T. Ooya, *Chemistry*, 2006, **12**, 6730-6737.
29 J. Li, X. Li, X. P. Ni, X. Wang, H. Z. Li and K. W. Leong, *Biomaterials*, 2006, **27**, 4132-4140.
30 J. Li and X. J. Loh, *Adv. Drug Deliv. Rev.*, 2008, **60**, 1000–1017.
31 D. Ma, H. B. Zhang, K. Tua and L. M. Zhang, *Soft Matter*, 2012, **8**, 3665-3672.
32 H. Gao, Y. N. Wang, Y. G. Fan and J. B. Ma, *J. Control. Release*, 2006, **112**, 301-311.
33 H. Gao, Y. N. Wang, Y. G. Fan and J. B. Ma, *Bioorg. Med. Chem.*, 2006, **14**, 131-137.
34 H. Gao, Y. N. Wang, Y. G. Fan and J. B. Ma, *J. Control. Release,* 2005, **107**, 158-173.
35 S. Heino, S. Lusa, P. Somerharju, C. Ehnholm, V. M. Olkkonen and E. Ikonen, *P. Natl. Acad. Sci. U.S.A.,* 2000, **97**, 8375-8380.
36 A. K. Jain, A. K. Goyal, P. N. Gupta, K. Khatri, N. Mishra, A. Mehta, S. Mangal and S. P. Vyas, *J. Control. Release*, 2009, **136**, 161-169.
37 C. Chen, C. H. Yu, Y. C. Cheng, P. H. Yu and M. K. Cheung, *Biomaterials*, 2006, **27**, 4804-4814.
38 S. Roweton, S. J. Huang and G. Swift, *J. Environ. Polym. Degrad.*, 1997, **5**, 175-181.
39 H. J. Lee and Y. S. Bae, *Biomacromolecules*, 2011, **12**, 2686-2696.
40 T. Suma, K. Miyata, Y. Anraku, S. Watanabe, R. J. Christie, H. Takemoto, M. Shioyama, N. Gouda, T. Ishii, N. Nishiyama and K. Kataoka, *ACS Nano*, 2012, **6**, 6693-6705.
41 H. J. Gao, J. Xiong, T. J. Cheng, J. J. Liu, L. P. Chu, J. F. Liu, R. J. Ma and L. Q. Shi, *Biomacromolecules*, 2013, **14**, 460-467.
42 S. Takae, K. Miyata, M. Oba, T. Ishii, N. Nishiyama, K. Itaka, Y. Yamasaki, H. Koyama and K. Kataoka, *J. Am. Chem. Soc.*, 2008, **130**, 6001-6009.
43 W. F. Dong, A. Kishimura, Y. Anraku, S. Chuanoi and K. Kataoka, *J. Am. Chem. Soc.*, 2009, **131**, 3804-3805.
44 T. Kaneko, S. Tanaka, A. Ogura and M. Akashi, *Macromolecules*, 2005, **38**, 4861-4867.
45 C. P. Russell, S. S. Jeffrey, T. S. Christopher, G. Kumaravel and F. T. Lin, *J. Am. Chem. Soc.*, 1990, **112**, 3860-3868.
46 Y. Y. Liu, X. D. Fan and L. Gao, *Macromol. Biosci.*, 2003, **3**, 715-719.
47 M. Tomida, T. Nakato, S. Matsunami and T. Kakuchi, *Polymer*, 1997, **38**, 4733-4736.
48 G. Caldwell, E. W. Neuse and A.G. Perlwitz, *J. Appl. Polym. Sci.*, 1997, **66**, 911-919.
49 J. J. Sedmak and S. E. Grossberg, *Anal. Biochem.*, 1977, **79**, 544-552.
50 H. Liu, X. Z. Jiang, J. Fan, G. H. Wang and S. Y. Liu, *Macromolecules*, 2007, **40**, 9074-9083.
51 G. Mantovani, F. Lecolley, L. Tao, D. M. Haddleton, J. Clerx, J. Cornelissen and K. Velonia, *J. Am. Chem. Soc.*, 2005, **127**, 2966-2973.
52 A. P. Vogt and B. S. Sumerlin, *Macromolecules*, 2006, **39**, 5286-5292.
53 J. Lee, E. C. Cho and K. Cho, *J. Control. Release*, 2004, **94**, 323-335.
54 J. Wang and M. Jiang, *J. Am. Chem. Soc*., 2006, **128**, 3703-3708.
55 L. Y. Qiu, L. Zhang, C. Zheng and R. J. Wang, *J. Pharm. Sci.*, 2011, **100**, 2430-2442.
56 T. Nozaki, Y. Maeda, K. Ito and H. Kitano, *Macromolecules*, 1995, **28**, 522-524.
57 L. Y. Qiu, R. J. Wang, C. Zheng, Y. Jin and L. Q. Jin, *Nanomedicine,* 2010, **5**, 193-208.
58 R. A. Siegel and R. Langer, *J. Control. Release*, 1990, **14**, 153-167.